

Supplementary Information

Real-time dissection of individual virion-triggered cortical actin dynamics for human immunodeficiency virus entry into resting CD4 T cells

Wen Yin^{a, b, ‡}, Wei Li^{a, ‡}, Qin Li^a, Yuanyuan Liu^{a, b}, Ji Liu^{a, b}, Min Ren^{a, b}, Yingxin Ma^a, Zhiping Zhang^a, Xiaowei Zhang^a, Yuntao Wu^d, Shibo Jiang^e, Xian-En Zhang^c and Zongqiang Cui^{a,*}

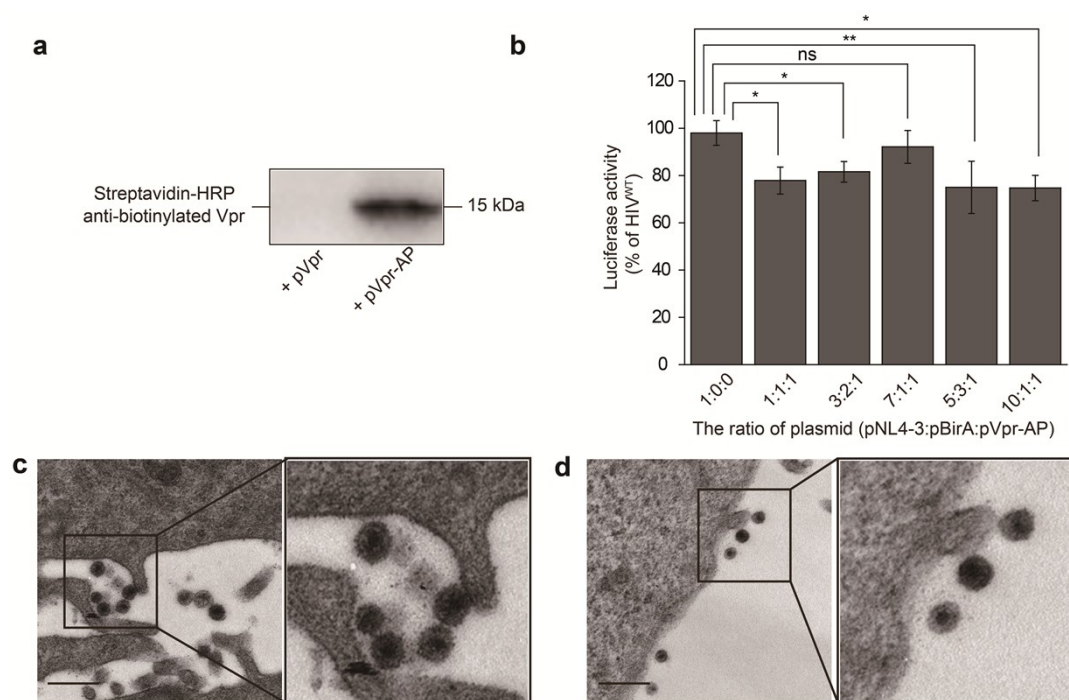


Fig. S1 Construction and characterization of QD-labeled HIV-1. (a) The biotinylation of the Vpr protein expressed in 293T cells were analyzed by western blotting. (b) Virus infectivity assay of QD-labeled HIV-1. TZM-bl cells (1×10^4) were cultured in 96-well plates for 24 h before infection and then infected with virions (dose equivalent to 100 ng of p24) in the presence of $15 \mu\text{g mL}^{-1}$ of DEAD dextran. Luciferase activity

was measured by end-point dilution 48 h after infection using the firefly luciferase reporter gene assay kit. Data are shown as the mean \pm SD of three independent experiments by analysis of Student's t test. * $p < 0.05$, ** $p < 0.01$, *ns*, not significant. (c, d) 293T cells producing HIV-1 NL4-3 and HIV-1-QDs were harvested at 48 h post-transfection, prepared, and analyzed by ultrathin section electron microscopy. (c) TEM imaging of ultrathin sectioned HIV-1 NL4-3 produced cells. Right panel is an enlargement view of the rectangular region. Scale bar, 500 nm. (d) TEM imaging of ultrathin sectioned HIV-1-QDs produced cells. Right panel is an enlargement view of the rectangular region. Scale bar, 500 nm.

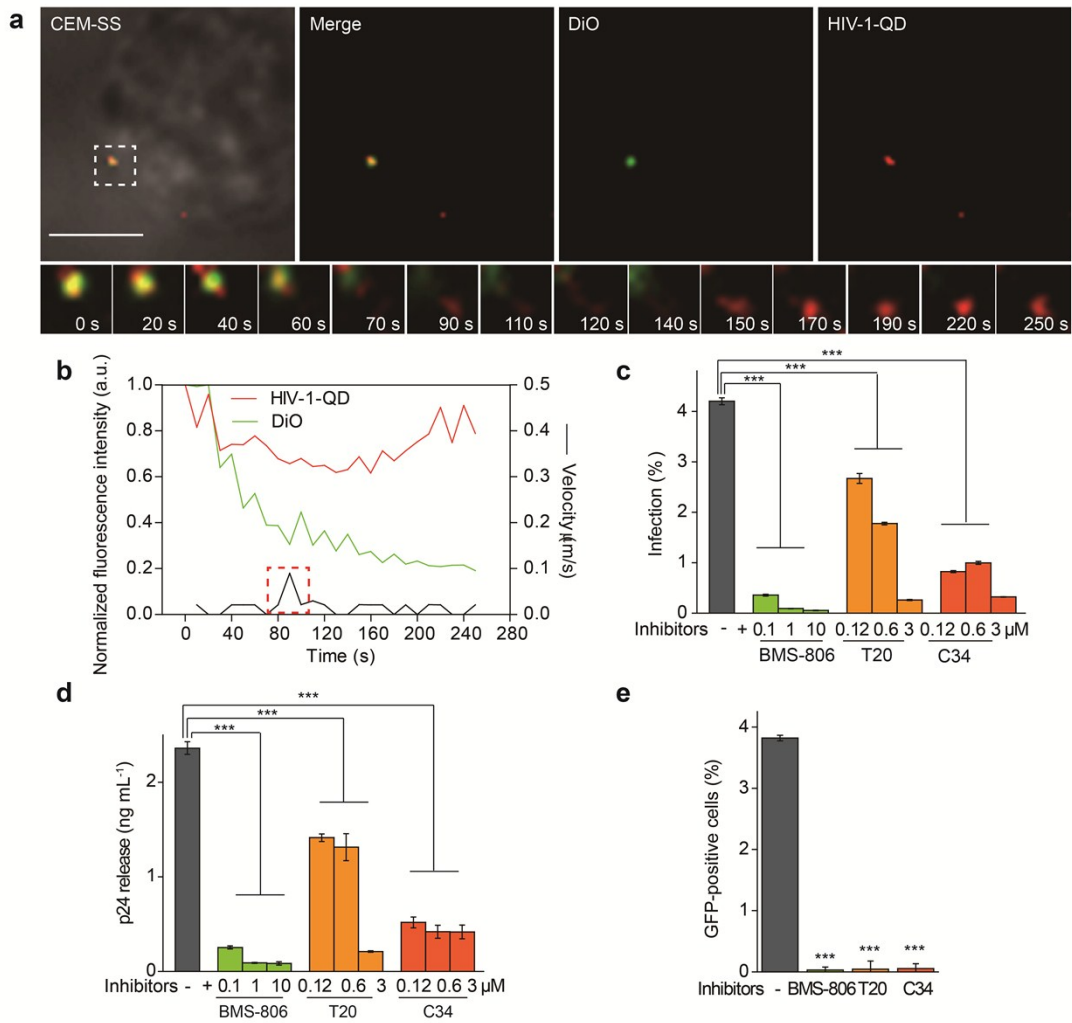


Fig. S2 Real-time imaging of HIV-1 cellular membrane fusion in CEM-SS cells. (a) Time-lapse images of dual-fluorescence-labeled HIV-1 particle in CEM-SS (shown in the rectangular region). HIV-1 viruses co-labeled with DiO (green) and SA-QDs (red) are pseudocolored yellow. Scale bar, 5 μm . (b) Velocity and fluorescence intensity analysis of HIV-1 particle that was shown in (a). The red dashed rectangle marks the instantaneous velocity increase during viral separation. (c) Intracellular p24 was stained with an anti-p24 antibody and measured by flow cytometry. (d) The p24 release level in the supernatant was monitored by p24 ELISA. (e) Viral infection was monitored by flow cytometry analysis of HIV-dependent GFP expression in Rev-CEM cells. Histograms display averages \pm SD; $n = 3$; *** $p < 0.001$.

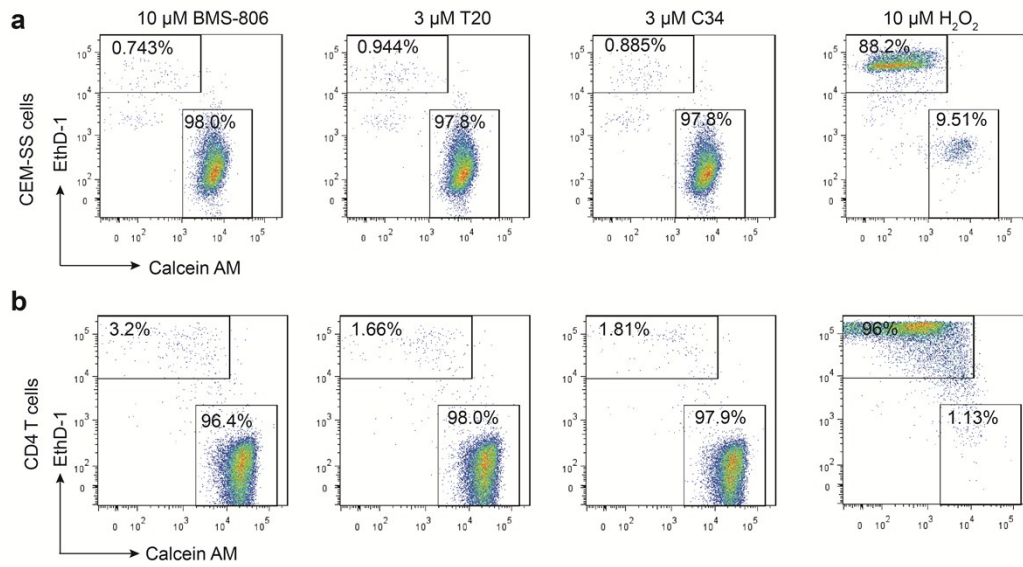


Fig. S3 Cytotoxic effect of inhibitors on different cells. CEM-SS cells (a), CD4 T cells (b) were exposed to different inhibitors at the desired concentrations, or 10 μ M H₂O₂ for 4 h. Then, the media was removed and a LIVE/DEAD[®] Viability/Cytotoxicity Kit was used to analysis the cell toxicity (live cells: green, dead cells: red).

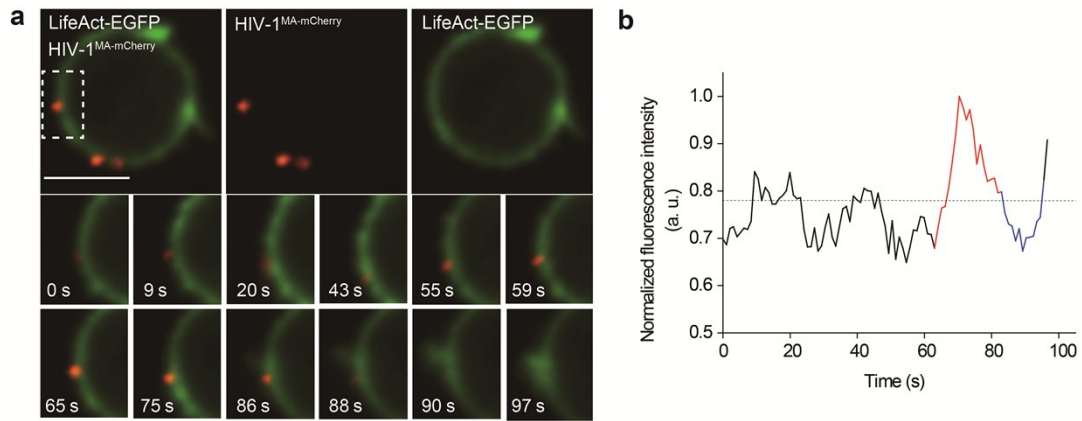


Fig. S4 Real-time imaging of cortical actin rearrangement upon HIV-1^{MA-mCherry} binding. (a) Real-time imaging of the HIV-1 entry triggered cellular actin arrangement. Scale bar, 5 μm . (b) Fluorescence intensity analysis of LifeAct-EGFP during HIV-1 entry that was shown in (a). Blue and red curves represent the rapid clustering and diffusion of F-actin, respectively. Black curve represents the normal arrangement of actin. The black dashed line indicates the baseline fluorescent intensity.

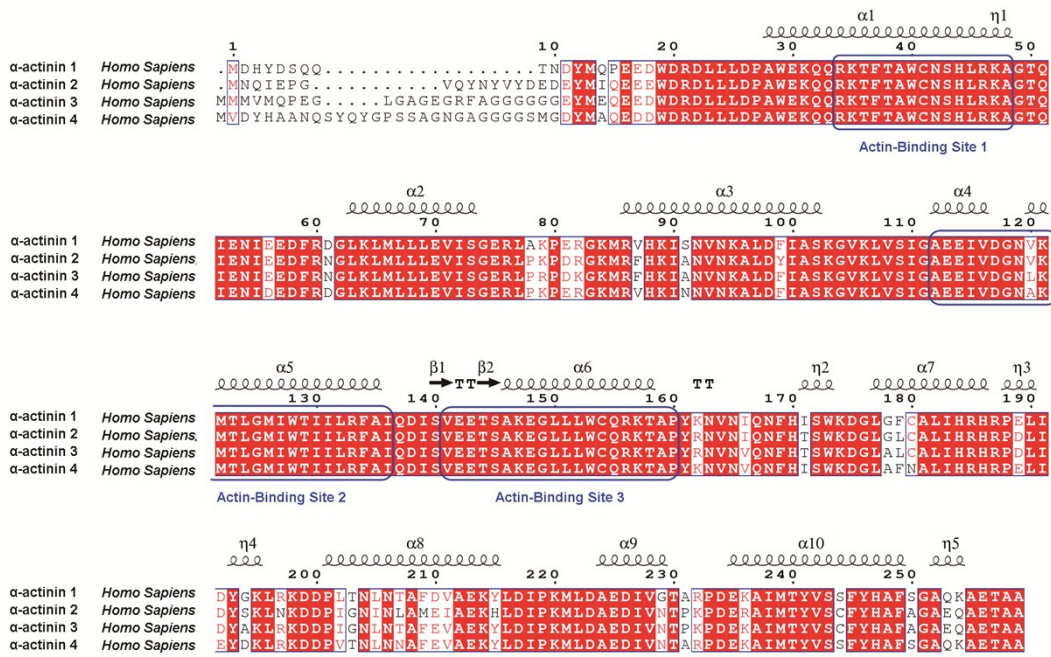


Fig. S5 Structure-based sequence alignments of ABD from *Homo sapiens* α -actinins. The sequences are annotated with the corresponding secondary structures. Arrows represent β -strands, and helices represent helices. The conserved residues are colored in red. The ABSs are marked with blue boxes.

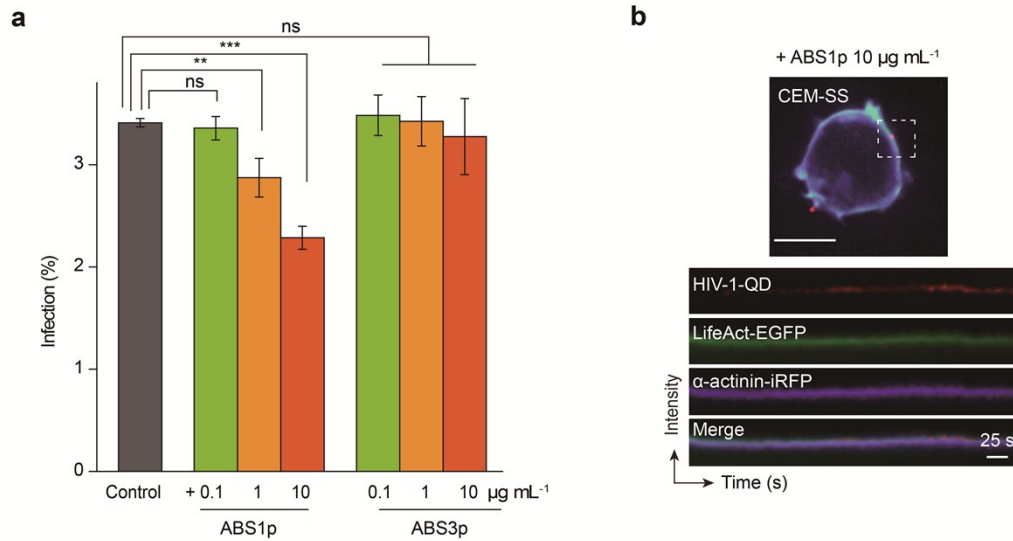


Fig. S6 α -Actinin-derived peptides can block HIV-1 entry and infection in CEM-SS cells. (a) Intracellular p24 was analyzed by flow cytometry after treatment with the ABS1p and ABS3p. Histograms display averages \pm SD; n = 3; **p < 0.01; ***p < 0.001; ns: no significant difference. (b) Kymograph analysis of the relationship between actin dynamics during HIV-1 entry after treatment with ABS1p. Scale bar, 5 μ m.

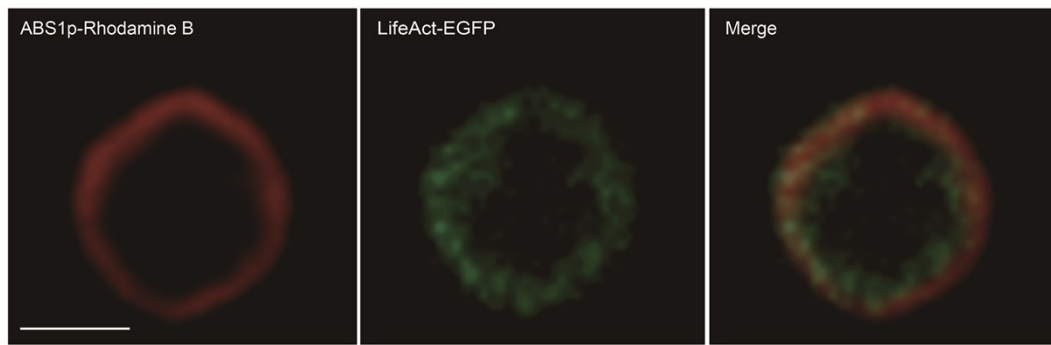


Fig. S7 Colocalization of ABS1p-Rhodamine B with LifeAct-EGFP in a CD4 T cell. ABS1p-Rhodamine B colocalized with LifeAct-EGFP marked F-actin are shown in a CD4 T cell. Cells were pretreated with ABS1p for 1 h at 37°C. Fluorescence was imaged with an UltraView VoX spinning disk confocal system (PerkinElmer Co.) using a Nikon Ti-e microscope with a 60 × objective lens. Scale bar, 5 μ m.

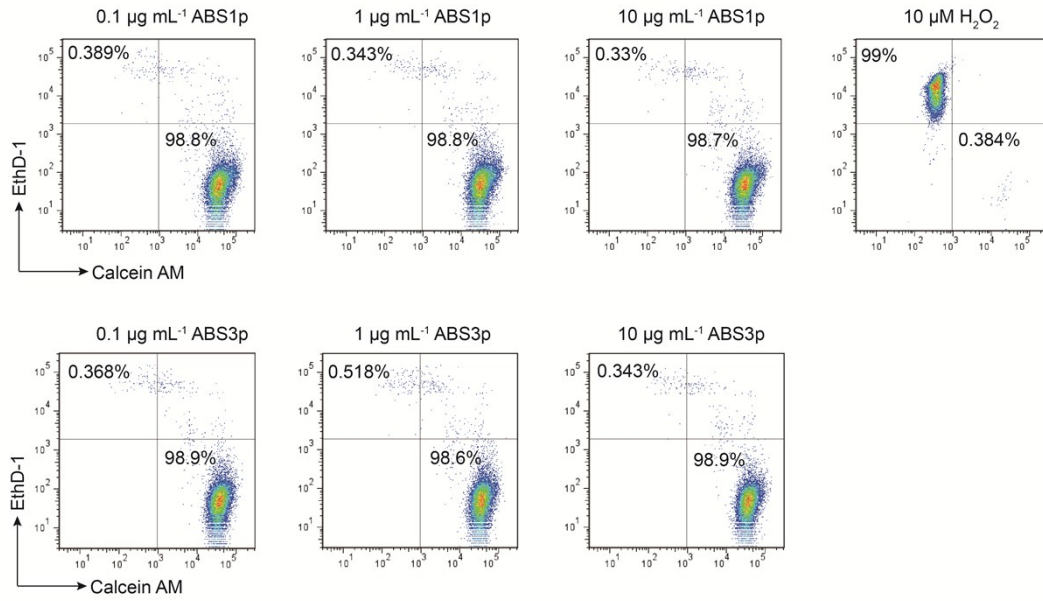


Fig. S8 Cytotoxic effect of peptides on CD4 T cells. The CD4 T cells were treated with different concentrations of ABS1p or ABS3p for 4 h, and the cell toxicity was analyzed by a LIVE/DEAD® Viability/Cytotoxicity kit. The cytotoxicities of these peptides were compared with the positive cytotoxic group, which were pretreated with 10 µM H₂O₂.

Video files:

Video S1. Real-time imaging of HIV-1-QD-DiO particle entry into CD4 T cells via fusion with cellular membrane. CD4 T cells were infected with HIV-1-QD-DiO. Fluorescence was imaged with an UltraView VoX spinning disk confocal system (PerkinElmer, Co.). Sequential images were taken at 10 s intervals for 430 s, and the video frame rate is 6 frames per second (fps). HIV-1-QD-DiO (yellow) was adsorbed to the cell membrane at the beginning, then the viral core (QD signal: red) was separated from the viral envelope (DiO signal: green) at the cell surface, and transported into the cytoplasm. Scale bar, 1 μm .

Video S2. Real-time imaging of T20 inhibition of HIV-1-QD-DiO particle entry into CD4 T cells. CD4 T cells were infected with HIV-1-QD-DiO. Fluorescence was imaged with an UltraView VoX spinning disk confocal system (PerkinElmer Co.). Sequential images were taken at 10 s intervals for 1667 s, and the video frame rate is 15 fps. HIV-1-QD-DiO (yellow) was attached to the cell membrane and could not enter the CD4 T cell during real-time imaging. Scale bar, 1 μm .

Video S3. Real-time imaging of HIV-1-QD-DiO particle entry into CEM-SS cells. CEM-SS cells were infected with HIV-1-QD-DiO. Fluorescence was imaged with an UltraView VoX spinning disk confocal laser scanning system (PerkinElmer Co.). Sequential images were taken at 10 s intervals for 279 s, and the video frame rate is 6 fps. HIV-1-QD-DiO (yellow) was adsorbed to the cell membrane at the beginning, and then the viral core (QD signal: red) was separated from the viral envelope (DiO signal: green) at the cell surface and internalized into the cytoplasm. Scale bar, 0.5 μm .

Video S4. Real-time imaging of the actin involving in the HIV-1-QD particle entry into CD4 T cells. CD4 T cells were labeled with a LifeAct-EGFP (green), and infected with HIV-1-QDs (red). Fluorescence was imaged with an UltraView VoX spinning disk confocal system (PerkinElmer Co.). Sequential images were taken at 6 s intervals for 342 s, and the video frame rate is 6 fps. HIV-1-QD (red) binding triggered rapid actin polymerization and depolymerization, and promoted the formation of a cap-like cluster and pore-like channel of F-actin (green). Scale bar, 1 μm .

Video S5. Real-time imaging of the actin involving in the mCherry labeled HIV-1 particle entry into CD4 T cells. CD4 T cells were labeled with a LifeAct-EGFP (green), and infected with mCherry labeled HIV-1 (red). Fluorescence was imaged with an UltraView VoX spinning disk confocal system (PerkinElmer Co.). Sequential images were taken at 1 s intervals for 120 s, and the video frame rate is 6 fps. mCherry labeled HIV-1 (red) binding triggered rapid actin polymerization and depolymerization, and promoted the formation of a cap-like cluster and pore-like channel of F-actin (green). Scale bar, 0.5 μm

Video S6. Real-time imaging of the actin involving in HIV-1-QD-DiO viral core release from the viral membrane in CD4 T cells. CD4 T cells were transiently transfected with a LifeAct-ECFP (cyan) expression vector, infected with HIV-1-QD-DiO (yellow). Fluorescence was imaged with an UltraView VoX spinning disk confocal system (PerkinElmer Co.). Sequential images were taken at 10 s intervals for 570 s, and the video frame rate is 6 fps. HIV-1-QD-DiO binding triggered F-actin to form a cap-like aggregation, then we observed a separation of the viral envelope (DiO signal: green) and viral core (QD signal: red). Following the separation, the actin

capping area (cyan) diffused, and a pore-like channel formed, the viral core (QD signal: red) passed through the cortical actin layer and was transported into the cytoplasm. Scale bar, 5 μm .

Video S7. Real-time imaging of the α -actinin involving in HIV-1-QD entry into CD4 T cells. CD4 T cells were transiently transfected with a LifeAct-EGFP (green) and α -actinin-iRFP (purple) expression vector, infected with HIV-1-QD (red). Fluorescence was imaged with an UltraView VoX spinning disk confocal system (PerkinElmer Co.). Sequential images were taken at 2.6 s intervals for 153 s, and the video frame rate is 6 fps. HIV-1-QD binding triggered α -actinin recruitment (purple), and the cortical actin filaments (green) diffused to form a channel at the viral entry site. Following HIV-1-QD (red) across the cortical actin layer, the α -actinin (purple) dispersed, and the channel was filled by the polymerized F-actin (green). Scale bar, 1 μm .

Video S8. Real-time imaging of the arrangement of cortactin and actin with HIV-1-QD entry into CD4 T cells. CD4 T cells were transiently transfected with a LifeAct-EGFP (green) and cortactin-iRFP (purple) expression vector. Fluorescence was imaged with an UltraView VoX spinning disk confocal system (PerkinElmer Co.). Sequential images were taken at 7.5 s intervals for 180 s, and the video frame rate is 6 fps. The cortactin (purple) and the cortical actin filaments (green) showed a similar rearrangement. Scale bar, 0.5 μm .

Video S9. Real-time imaging of the arrangement of paxillin and actin with HIV-1-QD entry into CD4 T cells. CD4 T cells were transiently transfected with a LifeAct-EGFP (green) and paxillin-iRFP (purple) expression vector. Fluorescence was

imaged with an UltraView VoX spinning disk scanning system (PerkinElmer Co.). Sequential images were taken at 7.5 s intervals for 143 s, and the video frame rate is 6 fps. The paxillin (purple) and the cortical actin filaments (green) showed a similar rearrangement. Scale bar, 0.5 μm .

Video S10. Real-time imaging of the arrangement of α -actinin and actin without HIV-1-QD entry into CD4 T cells. CD4 T cells were transiently transfected with a LifeAct-EGFP (green) and α -actinin-iRFP (purple) expression vector. Fluorescence was imaged with an UltraView VoX spinning disk confocal system (PerkinElmer Co.). Sequential images were taken at 6 s intervals for 864 s, and the video frame rate is 15 fps. The α -actinin (purple) and the cortical actin filaments (green) showed a similar rearrangement. Scale bar, 1 μm .

Video S11. Real-time imaging of the arrangement of α -actinin and F-actin with HIV-1-QD entry into CEM-SS cells under treatment with ABS1p. CEM-SS cells were transiently transfected with a LifeAct-ECFP (cyan) and α -actinin-iRFP (purple) expression vector. Fluorescence was imaged with an UltraView VoX spinning disk confocal system (PerkinElmer Co.). Sequential images were taken at 4 s intervals for 998 s, and the video frame rate is 15 fps. The α -actinin (purple) and the cortical actin filaments (green) showed a similar rearrangement under treatment with ABS1p. Scale bar, 1 μm .

Video S12. Real-time imaging of the arrangement of α -actinin and F-actin with HIV-1-QD entry into CD4 T cells under treatment with ABS1p. CD4 T cells were transiently transfected with a LifeAct-EGFP (green) and α -actinin-iRFP (purple) expression vector. Fluorescence was imaged with an UltraView VoX spinning disk

confocal system (PerkinElmer Co.). Sequential images were taken at 2.8 s intervals for 360 s, and the video frame rate is 6 fps. The treatment of ABS1p affected the sequential rearrangement pattern of α -actinins (purple) and F-actin (green). Scale bar, 0.5 μm .